cases of slow relaxation in the presence of applied magnetic fields have been demonstrated for a number of distorted octahedral Fe(II) compounds.[15,16] More unusual is the observation of slow relaxation in zero magnetic field. In addition to this study that extends the examples of slow relaxation in zero magnetic field, we have recently reported a study of slow paramagnetic relaxation in the monomeric, pseudotetrahedral complexes Fe(2,9-$(CH_3)_2$-1,10-phen)$(NCS)_2$ and Fe(2,9-$(CH_3)_2$-4,7-Ph_2-1,10-phen)$(NCS)_2$.[17] It is hoped that further studies of the latter coordination systems will give a better understanding of the nature of slow paramagnetic relaxation for high-spin Fe^{2+}.

Acknowledgment. This research was supported by the NSF, Grant No. DMR-77-12625. The authors also thank Professor A. K. Gregson for communicating his magnetic susceptibility results prior to publication.

Registry No. $Fe(acac)_2$, 14024-17-0.

(15) D. C. Price, C. E. Johnson, and I. Maartense, *J. Phys. C*, **10**, 4843 (1977).
(16) C. Nicolini, J. Chappert, and J. P. Mathieu, *Inorg. Chem.*, **16**, 3112 (1977), and references therein.
(17) W. M. Reiff, C. Nicolini, and B. Dockum, *J. Phys. (Orsay, Fr.)*, **40**, C2-230 (1978).

Contribution from the Department of Chemistry, Karl Marx University, 701 Leipzig, GDR

Single-Crystal EPR Studies on Nickel(III), Palladium(III), and Platinum(III) Dithiolene Chelates Containing the Ligands Isotrithionedithiolate, *o*-Xylenedithiolate, and Maleonitriledithiolate

REINHARD KIRMSE,* JOACHIM STACH, WOLFGANG DIETZSCH, GÜNTER STEIMECKE, and EBERHARD HOYER

Received June 18, 1979

Single-crystal EPR studies of the tetra-*n*-butylammonium salts of bis(isotrithionedithiolato)nickelate(III), -palladate(III), and -platinate(III), bis(maleonitriledithiolato)nickelate(III), and bis(*o*-xylenedithiolato)nickelate(III) and -palladate(III), diamagnetically diluted in the corresponding Cu(III) or Au(III) complexes, are reported. Enrichment of the magnetic isotope of nickel (^{61}Ni) has been used in order to determine the nickel hyperfine tensor. Satellite lines due to hyperfine coupling of the electron spin with naturally abundant ^{33}S were observed in the spectra of most of the chelates studied. The ^{33}S hyperfine structure data support a b_{2g} ground state in which the half-filled out-of-plane π molecular orbital is extensively delocalized over the ligands. The spin-Hamiltonian parameters of the bis(maleonitriledithiolato)nickelate(III) monoanion have been calculated from the results of extended Hückel molecular orbital calculations. These calculations confirm the b_{2g} ground state but difficulties arise in the explanation of the full set of the experimentally obtained EPR parameters. Several general conclusions concerning the EPR parameters and the metal–ligand bonds of the d^7 low-spin chelates studied have been derived from the experimental data. The electron spin–lattice relaxation was studied for the bis(maleonitriledithiolato)nickelate(III) monoanion in the temperature range $1.5 \leq T \leq 20$ K. Spin–lattice interactions were found to be mainly responsible for the small line widths observed in the spectra. The synthesis of the tetra-*n*-butylammonium salts of the new chelates bis(isotrithionedithiolato)nickelate(III), -palladate(III), -platinate(III), and -aurate(III) is reported.

Introduction

Dithiolene ligands are known to form transition-metal complexes in which unusual oxidation states of the metal ions are stabilized.[1-5] During the last years single-crystal EPR studies were made on the dithiolene chelates $[Ni(mnt)_2]^-$,[6,7] $[Rh(mnt)_2]^{2-}$,[6] and $[Au(mnt)_2]^{2-}$[8-10] (mnt = maleonitriledithiolate) which contain the metals in the oxidation states Ni(III), Rh(II), and Au(II), respectively. Recently we reported the single-crystal EPR spectra for $[Pd(mnt)_2]^-$[11] and $[Pt(mnt)_2]^-$.[12] Some other dithiolene chelates containing three-valent nickel, palladium, or platinum were studied by means of EPR in liquid or frozen solutions only.[13-18] The unusually small line widths observed in the single-crystal EPR

(1) J. A. McCleverty, *Prog. Inorg. Chem.*, **10**, 49 (1968).
(2) (a) G. N. Schrauzer, *Transition Met. Chem.*, **4**, 299 (1968); (b) G. N. Schrauzer, *Acc. Chem. Res.*, **2**, 72 (1969).
(3) E. Hoyer, W. Dietzsch, and W. Schroth, *Z. Chem.*, **11**, 41 (1971).
(4) W. E. Geiger, Jr., C. S. Allen, T. E. Mines, and F. C. Senftleber, *Inorg. Chem.*, **16**, 2003 (1977).
(5) R. Kirmse, J. Stach, and W. Dietzsch, *Inorg. Chim. Acta*, **29**, L 181 (1978).
(6) A. H. Maki, N. Edelstein, A. Davison, and R. H. Holm, *J. Am. Chem. Soc.*, **86**, 4580 (1964).
(7) R. D. Schmitt and A. H. Maki, *J. Am. Chem. Soc.*, **90**, 2288 (1968).
(8) J. G. M. van Rens and E. de Boer, *Mol. Phys.*, **19**, 745 (1970).
(9) R. L. Schlupp and A. H. Maki, *Inorg. Chem.*, **13**, 44 (1974).
(10) J. G. M. van Rens, M. P. A. Viegers, and E. de Boer, *Chem. Phys. Lett.*, **28**, 104 (1974).
(11) R. Kirmse and W. Dietzsch, *J. Inorg. Nucl. Chem.*, **38**, 255 (1976).
(12) R. Kirmse, W. Dietzsch, and B. V. Solovev, *J. Inorg. Nucl. Chem.*, **39**, 1157 (1977).
(13) A. Davison, N. Edelstein, R. H. Holm, and A. H. Maki, *J. Am. Chem. Soc.*, **85**, 2029 (1963).
(14) A. Davison, N. Edelstein, R. H. Holm, and A. H. Maki, *Inorg. Chem.*, **3**, 814 (1964).
(15) E. Billig, S. I. Shupack, J. H. Waters, R. Williams, and H. B. Gray, *J. Am. Chem. Soc.*, **86**, 926 (1964).
(16) G. N. Schrauzer and V. P. Mayweg, *J. Am. Chem. Soc.*, **87**, 3585 (1965).
(17) R. Williams, E. Billig, J. H. Waters, and H. B. Gray, *J. Am. Chem. Soc.*, **88**, 43 (1966).
(18) A. V. Ryshmanova and N. S. Garif'yanov, *Zh. Neorg. Khim.*, **15**, 3095 (1970).

0020-1669/80/1319-2679$01.00/0

Table I. Analytical Data, Melting Points, and Magnetic Moments for $(n\text{-Bu}_4N)[M(dmi\text{-}t)_2]$ Complexes[a]

compd	analytical data: % calcd C	H	N	S	% found C	H	N	S	mp, °C	μ_{eff}, μ_B
$(n\text{-Bu}_4N)[Ni(dmi\text{-}t)_2]$	38.11	5.20	2.02	46.20	38.37	5.30	2.21	45.47	191	1.90
$(n\text{-Bu}_4N)[Pd(dmi\text{-}t)_2]$	35.66	4.86	1.89	43.22	35.61	4.62	1.97	43.56	207	1.74
$(n\text{-Bu}_4N)[Pt(dmi\text{-}t)_2]$	31.85	4.34	1.69	38.60	32.15	4.45	1.50	38.95	204	1.74
$(n\text{-Bu}_4N)[Au(dmi\text{-}t_2]$	31.77	4.33	1.69	38.51	31.38	4.35	1.54	38.70	221	

[a] The complexes were obtained in yields between 65 and 80%.

spectra of the mnt complexes and the interesting bonding properties of these covalent low-spin d^7 chelates have prompted us to study the dithiolene chelates tetra-*n*-butylammonium bis(isotrithionedithiolato)nickelate(III), $(n\text{-Bu}_4N)[Ni(dmi\text{-}t)_2]$ (I), tetra-*n*-butylammonium bis(isotrithionedithiolato)palladate(III), $(n\text{-Bu}_4N)[Pd(dmi\text{-}t)_2]$ (I), tetra-*n*-butylammonium bis(isotrithionedithiolato)platinate(III), $(n\text{-Bu}_4N)[Pt(dmi\text{-}t)_2]$ (I), tetra-*n*-butylammonium bis(*o*-xylenedithiolato)nickelate(III), $(n\text{-Bu}_4N)[Ni(xdt)_2]$ (II), and tetra-*n*-butylammonium bis(*o*-xylenedithiolato)palladate(III), $(n\text{-Bu}_4N)[Pd(xdt)_2]$ (II), by means of the single-crystal EPR technique. These chelates were expected to provide detailed information about the bonding properties in nickel(III), palladium(III), and platinum(III) dithiolene chelates because of the strong differences in the structure and the electronic properties of the studied ligand types with respect to the maleonitriledithiolate ligand.

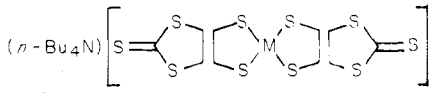

$M = Ni^{3+}, Pd^{3+}, Pt^{3+}$

I

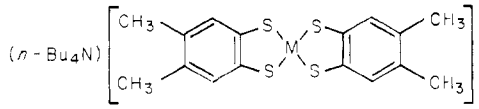

$M = Ni^{3+}, Pd^{3+}$

II

The $[M(dmi\text{-}t)_2]^-$ complexes represent a new class of dithiolene compounds. Therefore, their synthesis will be described in the Experimental Section in detail. The ligand dmi-t was obtained in our laboratory by an original synthesis directly from the reaction of carbon disulfide with alkali metals.[19,20]

The small line widths observed in the single-crystal spectra allow investigation of the magnetic nuclear hyperfine interactions due to ^{61}Ni and ^{105}Pd which are usually difficult to be resolved because of their small splitting. In order to get the complete ^{61}Ni hyperfine tensor, we used ^{61}Ni-enriched Ni complexes. From this point of view we reinvestigated the ^{61}Ni data for $[Ni(mnt)_2]^-$ (III) studied first by Maki et al.[6]

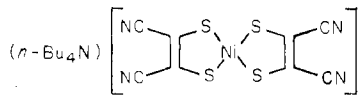

III

Furthermore, ^{33}S ligand hyperfine interactions could be resolved in the spectra in natural abundance ($^{33}S = 0.74\%$, $I = {}^3/_2$) providing direct information about the nature of the electronic ground state and the extent of electron spin delocalization over the ligand orbitals.

In order to understand the bonding situation in these complexes, we calculated the spin-Hamiltonian parameters for $[Ni(mnt)_2]^-$ by means of the iterative extended Hückel MO method (EHT–SCCC–LCAO–MO method) and compared these with the experimentally measured EPR quantities. In this way all metal and ligand orbitals are included.

Finally, the temperature dependence of the electron spin–lattice relaxation rate was studied on $(n\text{-Bu}_4N)[Ni/Au(mnt)_2]$ single crystals in order to explain the small EPR line widths observed in the spectra. As for our knowledge up to now, there are no results concerning the electron spin–lattice relaxation of Ni^{3+} in covalent chelates.

Experimental Section

Preparation of Complexes. $(n\text{-Bu}_4N)[M(dmi\text{-}t)_2]$, M = Ni, Pd, Pt. These compounds could be prepared following two different ways: (a) oxidation of $(n\text{-Bu}_4N)_2[M(dmi\text{-}t)_2]$ by iodine and (b) autoxidation of $(n\text{-Bu}_4N)_2[M(dmi\text{-}t)_2]$.

Method a. $(n\text{-Bu}_4N)_2[M(dmi\text{-}t)_2]$,[19,20] 1 mmol, was dissolved in 60 mL of acetone. Dropwise addition of a solution of 0.127 g (0.5 mmol) of iodine and 0.2 g of NaI in 35 mL of acetone at room temperature yields a solution of the metal(III) complexes. The volume of the reaction mixture was then reduced under vacuum to 35 mL. After addition of the same volume of methanol, crystals of the M(III) chelates are obtained. The complex salts were recrystallized from acetone–isopropyl alcohol.

Method b. $(n\text{-Bu}_4N)_2[M(dmi\text{-}t)_2]$, 1 mmol, was dissolved in ca. 60 mL of acetone. Under fast stirring during 5 min, 30 mL of glacial acetic acid was added. This solution was concentrated under vacuum at room temperature until crystallization occurred. The so-obtained M(III) chelates are analytically pure without recrystallization.

Yields, analytical data, and magnetic moments are listed in Table I.

$(n\text{-Bu}_4N)[Au(dmi\text{-}t)_2]$. A solution of 0.812 g (2 mmol) of bis(benzoylthio)isotrithione,[20,21] $C_3S_5(COC_6H_5)_2$, in 20 mL of acetone was treated with 10 mL of concentrated NH_3 solution and stirred for 10 min. $HAuCl_4$, 0.9 mmol, dissolved in a mixture of 10 mL of acetone and 10 mL of methanol was added to the reaction mixture during a period of 15 min. To the yellow-brown solution obtained after filtration was added a solution of 0.372 g (1 mmol) of $n\text{-Bu}_4NI$ in 10 mL of methanol, followed by a treatment with a mixture of 10 mL of glacial acetic acid and 30 mL of methanol. The solution was concentrated under vacuum. Brown crystals of $(n\text{-Bu}_4N)[Au(dmi\text{-}t)_2]$ are obtained which could be recrystallized from acetone (see Table I).

$(n\text{-Bu}_4N)[Ni(xdt)_2]$ and $(n\text{-Bu}_4N)[Cu(xdt)_2]$ were prepared as described by Baker-Hawkes et al.[22]

$(n\text{-Bu}_4N)[Pd(xdt)_2]$ was not described in the literature. This chelate was synthesized according to the method described for the analogous Ni(III) chelate[22] and used for the preparation of single crystals without further purification.

$(n\text{-Bu}_4N)[Ni(mnt)_2]$ and $(n\text{-Bu}_4N)[Au(mnt)_2]$ were prepared as previously reported by Billig et al.[23]

For the preparation of ^{61}Ni-enriched Ni(III) complexes, $^{61}NiCl_2{\cdot}6H_2O$ (containing 70% ^{61}Ni) was used as the starting material.

Preparation of Single Crystals. Single crystals of $(n\text{-Bu}_4N)[Au(dmi\text{-}t)_2]$ containing approximately 1% of $(n\text{-Bu}_4N)[Ni(dmi\text{-}t)_2]$, $(n\text{-Bu}_4N)[Pd(dmi\text{-}t)_2]$, or $(n\text{-Bu}_4N)[Pt(dmi\text{-}t)_2]$, respectively, were

(19) G. Steimecke, R. Kirmse, and E. Hoyer, *Z. Chem.*, **15**, 28 (1975).
(20) G. Steimecke, Thesis, University of Leipzig, 1977.
(21) G. Steimecke, J. Sieler, R. Kirmse, and E. Hoyer, *Phosphorus Sulfur*, **7**, 49 (1979).
(22) M. J. Baker-Hawkes, E. Billig, and H. B. Gray, *J. Am. Chem. Soc.*, **88**, 4870 (1966).
(23) E. Billig, R. Williams, I. Bernal, J. H. Waters, and H. B. Gray, *Inorg. Chem.*, **3**, 663 (1964).

Table II. Single-Crystal EPR Parameters[a,b] for Nickel-Group mnt, dmi-t and xdt Complexes

paramagn chelate	host chelate	g_x	g_y	g_z	A_x	A_y	A_z	$A_x'^S$ (=$A_\parallel^S$)	$A_y'^S = A_z'^S$ (=$A_\perp^S$)
$Ni(mnt)_2^-$	$Au(mnt)_2^-$	2.042	2.156	1.996	−5.3	14.0	4.4	14.4	4.6
$Ni(mnt)_2^-$	$Cu(mnt)_2^-$ [c]	2.042	2.160	1.998	2.9	15.0	2.0	14.27	4.55
$Ni(dmi\text{-}t)_2^-$	$Au(dmi\text{-}t)_2^-$	2.041	2.105	2.001	−5.3	13.1	4.5	13.0	4.4
$Ni(xdt)_2^-$	$Cu(xdt)_2^-$	2.045	2.174	2.008	−5.0	12.5	4.0		
$Pd(mnt)_2^-$	$Au(mnt)_2^-$ [d]	2.043	2.071	1.956	5.9	10.3	5.4	16.8	5.8
$Pd(dmi\text{-}t)_2^-$	$Au(dmi\text{-}t)_2^-$	2.044	2.045	1.967	5.4	10.0	4.8	14.8	5.5
$Pd(xdt)_2^-$	$Cu(xdt)_2^-$	2.047	2.069	1.950	5.5	9.5	4.3	14.8	
$Pt(mnt)_2^-$	$Au(mnt)_2^-$ [e]	2.065	2.245	1.827	−125.5	0.0	−99.1	16.3	
$Pt(dmi\text{-}t)_2^-$	$Au(dmi\text{-}t)_2^-$	2.073	2.168	1.858	−99.2	−21.8	−78.1	–	

[a] Experimental errors: $g_i \pm 0.001$ $(i = x, y, z)$, $A_i \pm 0.2$ $(i = x, y, z)$, $A_x'^S \pm 0.2$, $A_y'^S$ $(=A_z'^S) \pm 0.5$. [b] Hyperfine coupling constants are given in 10^{-4} cm^{-1}. [c] Data taken from ref 7. [d] Data taken from ref 11. [e] Data taken from ref 12.

grown by slow evaporation of an acetone solution at room temperature. Single crystals of $(n\text{-}Bu_4N)[Au(mnt)_2]$ doped with approximately 1% of $(n\text{-}Bu_4N)[Ni(mnt)_2]$ as well as suitable crystals of $(n\text{-}Bu_4N)[Cu(xdt)_2]$ doped with ca. 0.1% of $(n\text{-}Bu_4N)[Ni(xdt)_2]$ or $(n\text{-}Bu_4N)[Pd(xdt)_2]$ were obtained in a similar manner by using $CHCl_3$ as the solvent. Attempts made to prepare diamagnetically diluted crystals with the host lattice $(n\text{-}Bu_4N)[Au(xdt)_2]$ were unsuccessful. Also, crystals containing $(n\text{-}Bu_4N)[Pt(xdt)_2]$ could not be obtained.

EPR Measurements. EPR spectra were recorded in the X band (at 9.5 GHz) by using a Varian E-112 spectrometer. The principal values of the **g** and the hyperfine splitting tensors were determined as described earlier.[11] Except for the system $(n\text{-}Bu_4N)[Ni/Au(mnt)_2]$ which has been studied at temperatures down to $T = 1.5$ K, all measurements were carried out at room temperature.

Relaxation Measurements. Measurements of the electron spin–lattice relaxation time T_1 were made on $(n\text{-}Bu_4N)[Ni/Au(mnt)_2]$ crystals containing 2–3% Ni^{3+} (relative to Au^{3+}). The relaxation data were obtained with a 28.8 GHz superheterodyne spectrometer as described earlier[24] in the temperature range $1.5 \leq T \leq 20$ K by using the pulse saturation technique. The pulse width was varied between 2 and 10 ms. The signal-klystron power entering the cavity was approximately 1 μW; the ratio of the power of the saturating pulses to the signal-klystron power was approximately 10^5.

Results

Crystal Structures. Crystal structure data of the host complexes $(n\text{-}Bu_4N)[Au(dmi\text{-}t)_2]$, $(n\text{-}Bu_4N)[Cu(xdt)_2]$, and $(n\text{-}Bu_4N)[Au(mnt)_2]$ have not been reported in the literature up to now. However, the general features of the angular dependence of the **g** tensors of both sites present in the unit cell of all systems studied in this work are very similar to those found for the system $(n\text{-}Bu_4N)[Ni/Cu(mnt)_2]$ by Schmitt and Maki.[6,7] Therefore, one may conclude that the crystal structures of the chelates $(n\text{-}Bu_4N)[Au(dmi\text{-}t)_2]$, $(n\text{-}Bu_4N)[Cu(xdt)_2]$ and $(n\text{-}Bu_4N)[Au(mnt)_2]$ have some similarities with respect to that of $(n\text{-}Bu_4N)[Cu(mnt)_2]$[25] which has a monoclinic unit cell with 8 formula units.

From Weissenberg photographs made in our department[26] $(n\text{-}Bu_4N)[Au(mnt)_2]$ was found to be isomorphous with $(n\text{-}Bu_4N)[Cu(mnt)_2]$. As found for the copper compound, $(n\text{-}Bu_4N)[Au(mnt)_2]$ also crystallizes monoclinic, space group $I2/c$, with 8 formula units in the unit cell. The unit cell dimensions are $a = 16.52$ Å, $b = 14.47$ Å, and $c = 28.15$ Å with the monoclinic angle $\beta = 96°$. Recently Noordik and Beurskens[27] reported the structure of the complex $[Au(n\text{-}Bu_2dtc)_2][Au(mnt)_2]$ from which structural data for the formula unit $[Au(mnt)_2]^-$ are available (n-Bu_2dtc = *N*,*N*-di-*n*-butyldithiocarbamate). The central part of the $[Au(mnt)_2]^-$ unit is planar and has nearly D_{4h} symmetry; the Au atom occupies an inversion center.

Table III. Experimentally Obtained and Calculated EPR Parameters[a] for $(n\text{-}Bu_4N)[Ni/Au(mnt)_2]$

	exptl	calcd
g_{zz}	1.996	2.037
g_{yy}	2.156	2.225
g_{xx}	2.042	2.004
$A_{zz}^{Ni} - A_{av}^{Ni}$	0.0	0.1
$A_{yy}^{Ni} - A_{av}^{Ni}$	9.6	2.9
$A_{xx}^{Ni} - A_{av}^{Ni}$	−9.7	−2.8
A_{av}^{Ni}	4.4	
$A_{z'}^{S} - A_{av}^{S}$	−3.27	−4.55
$A_{y'}^{S} - A_{av}^{S}$	−3.27	−4.55
$A_{x'}^{S} - A_{av}^{S}$	6.53	9.10
A_{av}^{S}	7.87	

[a] Hyperfine splittings in 10^{-4} cm^{-1}.

Of the paramagnetic complexes studied structural data are available for $(Et_4N)[Ni(mnt)_2]$[28] only. Despite the fact that the structures of the guest and the host complexes may be different ones the single-crystal EPR spectra show that the incorporated paramagnetic complexes accept the structure of the diamagnetic host complexes.

EPR Spectra. Generally the EPR spectra show the signals of two magnetically nonequivalent molecules for all the single crystals studied. From the angular dependences of the spectra a rotation axis can be easily found for which both molecular units are magnetically equivalent. When the crystals are rotated around this axis, the direction of the minimum **g**-tensor component (denoted by g_z) comes within $(4 \pm 2)°$ of being coincident with the magnetic field direction. The same was observed for the $[Ni/Cu(mnt)_2]^-$ system.[7] Therefore, this rotation axis can be assumed as being identical with the crystallographic b axis.

For all systems studied the EPR spectra can be described by a rhombic-symmetric spin Hamiltonian

$$\hat{H}_{sp} = \beta_e \sum_{i=x,y,z} g_i H_i \hat{S}_i + \sum_{i=x,y,z} \hat{S}_i A_i^M I_i^M + \sum_{j=x',y',z'} \hat{S}_j A_j^S \hat{I}_j^S$$

where the first term describes the electron–Zeeman interaction and the second and the third term stands for the metal and the ^{33}S ligand hyperfine interaction (hfs), respectively ($\hat{S}_i$ and $\hat{I}_i$ are components of the electron and nuclear spin operators; β_e is the Bohr magneton; g_i, A_i^M, and A_j^S are components of the **g**, the metal hfs, and the ^{33}S hfs tensors, respectively). In all systems studied the principal axes of the **g** tensor coincide with those of the metal hfs tensor within the experimental error. The principal values of the **g** and the metal hfs tensors are collected in Table II.

The EPR spectra of ^{61}Ni-enriched $[Ni(dmi\text{-}t)_2]^-$, $[Ni(mnt)_2]^-$, and $[Ni(xdt)_2]^-$ show the expected ^{61}Ni hfs-line quartet caused by the interaction of the unpaired electron with the ^{61}Ni nuclei (^{61}Ni, $I = {}^3/_2$). The central line in the spectra

(24) R. Kirmse, B. V. Solovev, and B. G. Tarasov, *Z. Phys. Chem. (Leipzig)*, **255**, 711 (1974).
(25) J. D. Forrester, A. Zalkin, and D. H. Templeton, *Inorg. Chem.*, **3**, 1507 (1964).
(26) J. Sieler, private communication.
(27) J. H. Noordik and P. T. Beurskens, *J. Cryst. Mol. Struct.*, **1**, 339 (1971).
(28) A. Kobayashi and Y. Sasaki, *Bull. Chem. Soc. Jpn.*, **50**, 2650 (1977).

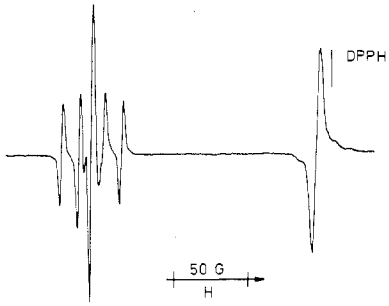

Figure 1. X-Band single-crystal EPR spectrum of $(n\text{-}Bu_4N)[^{61}Ni/Au(dmi\text{-}t)_2]$. The magnetic field is located parallel to the direction of the maximum **g** tensor component of one site of the unit cell. T = 295 K.

Figure 2. X-Band single-crystal EPR spectrum of $(n\text{-}Bu_4N)[^{61}Ni/Au(mnt)_2]$. The magnetic field is located perpendicular to the b axis (nearly coincident with the direction of g_z). T = 295 K.

is due to Ni complexes which contain the remaining Ni isotopes having a zero nuclear spin. Whereas for magnetic field directions around the maximum g value (g_y) the ^{61}Ni hfs appears to be well resolved, its resolution is bad in the region of the other two principal g values. Two representative spectra are reproduced in Figures 1 and 2.

For obtainment of the relative signs of the ^{61}Ni hfs tensor components, the EPR spectrum of $(n\text{-}Bu_4N)[^{61}Ni(mnt)_2]$ has been studied in acetone–dimethylformamide (1:1) at room temperature. From this the isotropic ^{61}Ni hfs coupling constant was found to be $a_0^{Ni} = (4.0 \pm 1.0) \times 10^{-4}$ cm^{-1}. This result was checked by computer simulation of the liquid solution spectrum with the use of the line width parameters found from the spectrum of $(n\text{-}Bu_4N)[Ni(mnt)_2]$ which contains ^{61}Ni in natural abundance. Averaging the ^{61}Ni hfs tensor components can obtain a good agreement with the isotropic ^{61}Ni coupling constant only if one of the small components of the ^{61}Ni hfs tensor has the opposite sign as the other two. A similar behavior was observed for $(n\text{-}Bu_4N)[Ni(dmi\text{-}t)_2]$ and $(n\text{-}Bu_4N)[Ni(xdt)_2]$ also.

The EPR spectra of the Pd complexes $(n\text{-}Bu_4N)[Pd(dmi\text{-}t)_2]$ and $(n\text{-}Bu_4N)[Pd(xdt)_2]$ show in addition to an intense line (77.8% of the Pd isotopes have a zero nuclear spin) a hfs line sextet caused by the interaction of the unpaired electron with the ^{105}Pd nuclei (^{105}Pd, $I = {}^5/_2$, natural abundance 22.2%).

The EPR spectra of $(n\text{-}Bu_4N)[Pt(dmi\text{-}t)_2]$ show in addition to an intense central line (66.3% of the Pt isotopes have a zero nuclear spin) a less intense line doublet due to hyperfine interactions with the ^{195}Pt nuclei (^{195}Pt, $I = {}^1/_2$, natural abundance 33.7%). The **g** as well as the ^{195}Pt tensor has pronounced rhombic symmetry.

There are differences concerning the EPR line widths of the chelates studied. The line width in the spectra of $(n\text{-}Bu_4N)[Pt/Au(dmi\text{-}t)_2]$ is larger by a factor 2–3 than those observed for the Ni(III) and Pd(III) chelates.

In addition to the metal hyperfine lines in the EPR spectra of $(n\text{-}Bu_4N)[Ni/Au(mnt)_2]$, $(n\text{-}Bu_4N)[Ni/Au(dmi\text{-}t)_2]$, $(n\text{-}Bu_4N)[Pd/Au(dmi\text{-}t)_2]$, and $(n\text{-}Bu_4N)[Pd/Cu(xdt)_2]$, two additional very weak lines were observed when the magnetic field is located parallel to the direction of g_z (which is assumed to be coincident with the molecular z axis). The intensity of these lines is approximately 0.5–0.7% of that of the major peaks depending on the degree of overlapping between the metal hfs lines and the central line which is due to the nuclei having a nuclear spin $I = 0$. This is in good agreement with the calculated intensity for ^{33}S ligand hfs lines in natural abundance. A representative spectrum showing the ^{33}S satellite lines is given in Figure 2. Besides the ^{33}S hfs lines in the spectra of these crystals other weak signals could be detected which are much more dependent on the orientation of the magnetic field than the ^{33}S lines. Furthermore, these lines showed a strong intensity dependence on the concentration of the paramagnetic ions. On this basis we propose that these lines are caused by electron spin–electron spin interactions in metal–metal pairs. Similar features have been observed also by Schmitt and Maki in the EPR spectra of $(n\text{-}Bu_4N)[Ni/Cu(mnt)_2]$.[7]

Since the splitting of the ^{33}S hfs lines is small, only the outer lines of the satellite quartet are observed. Furthermore, they could only be observed within angles of some degrees about the z axis (±40° for the nickel complexes, ±25° for the palladium complexes), since the splitting becomes too small to be resolved for orientations in which the magnetic field is closer to the molecular plane. Thus only the $A_{x'}{}^S$ value (maximum ^{33}S splitting) could be determined accurately. The x' direction of the ^{33}S tensor was found to be coincident with that of g_z. A result concerning the symmetry of the ^{33}S tensor can be obtained only for the Ni complexes since the angular dependence of the ^{33}S satellites can be analyzed over a relatively large range of orientations. In all spectra only one set of ^{33}S lines was ever observed for each site in the unit cell. Also, the satellite line widths were not changed noticeably. Within experimental error, therefore, the ^{33}S tensor is axially symmetric with the perpendicular components $A_{y'}{}^S = A_{z'}{}^S = A_\perp{}^S$ in the molecular plane. The ^{33}S hfs data derived from the spectra are collected in Table I.

^{33}S ligand hfs data could not be obtained for $(n\text{-}Bu_4N)[^{61}Ni/Cu(xdt)_2]$ and $(n\text{-}Bu_4N)[Pt/Au(dmi\text{-}t)_2]$. In the former case the signal-to-noise ratio was not large enough to allow the detection of such weak lines because of the smallness of the crystals available. For the latter system these satellites are obscured because the line width of the EPR signals is too large.

Electron Spin–Lattice Relaxation Measurements. In Figure 3 the relaxation data obtained for $(n\text{-}Bu_4N)[Ni/Au(mnt)_2]$ crystals are presented. At temperatures $T < 9$ K direct (one-phonon) relaxation processes are observed whose temperature dependence can be described by $T_1^{-1} = 1.2 \times 10^2 T$ (s^{-1}); T_1^{-1} is the electron spin–lattice relaxation rate and T the absolute temperature, respectively. At higher temperatures the relaxation is defined by Raman processes. The temperature dependence of the Raman relaxation rate can be approximated by a $T_1^{-1} \approx T^{4.3}$ law in the temperature interval studied.

For $T \ll \Theta_D$ (Θ_D = Debye temperature) the temperature dependence of the relaxation rate for isolated Ni^{3+} ions, having a Kramers doublet as the ground state, should be of the form $T_1^{-1} = AT + BT^9$ (A and B are constants). The deviation between the theoretically predicted and the experimentally

(29) S. A. Altshuler and B. M. Kozyrev, "Electron Paramagnetic Resonance of Transition Metal Compounds", Nauka, Moscow, 1972, Chapter 5.

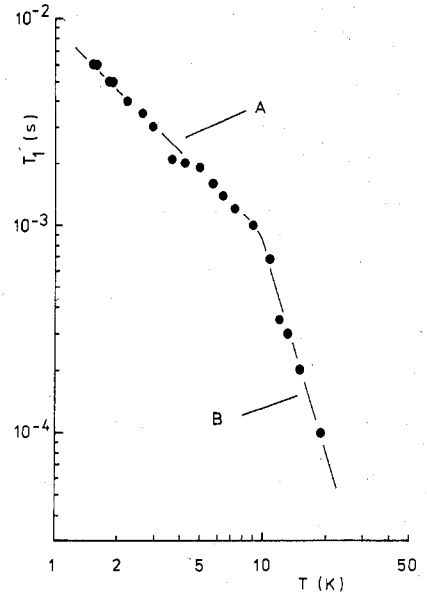

Figure 3. Electron spin–lattice relaxation data for (n-Bu_4N)[Ni/Au(mnt)$_2$] (Ni^{3+} concentration 3% relative to Au^{3+}): A, direct process $1/T_1 \approx T$; B, Raman process $1/T_1 \approx T^{4.3}$. H lies parallel to the molecular z axis.

measured temperature dependence of the Raman relaxation rate is caused obviously by the invalidity of $T \ll \Theta_D$ in the temperature range studied. Analogous results were obtained by us for several copper complexes which contain similar sulfur and selenium donor ligands[30-34] and seem to be typical for such molecular crystals. The Debye temperatures obtained for these crystals are found to be in the range $55 < \Theta_D < 110$ K and the calculated room-temperature line width contributions caused by spin–lattice interactions do not essentially exceed values of 1 G. Unfortunately, our attempts to get relaxation data for temperatures higher than 20 K were unsuccessful since we could not saturate the resonance lines. In general difficulties arise at low temperatures, because the crystals easily burst asunder in most cases. Nevertheless a rough estimation of the Debye temperature can be made according to the procedure described in detail by Kurkin et al.[35] yielding $\Theta_D = 80 \pm 20$ K for (n-Bu_4N)[Au(mnt)$_2$]. With this value, the room-temperature line width contribution caused by spin–lattice interactions was found to be 3 ± 2 G.

A relatively high concentration of the Ni chelate was used in order to perform directly relaxation measurements on Ni^{3+}–Ni^{3+} pair lines whose intensity should be large enough for such an experiment under these conditions. In all measurements made on the pair lines at $T = 4.2$ K we were not able to observe any noticeable saturation. Therefore, the pair relaxation rate T_1^{-1} is considerably greater than the "single ion" relaxation rate.

Molecular Orbital Calculations. Two different MO studies were reported by Gray et al.[17,36] and Schrauzer et al.[16] on nickel dithiolene compounds. Gray's calculations for [Ni(mnt)$_2$]$^-$ resulted in an a_g state for the unpaired electron.

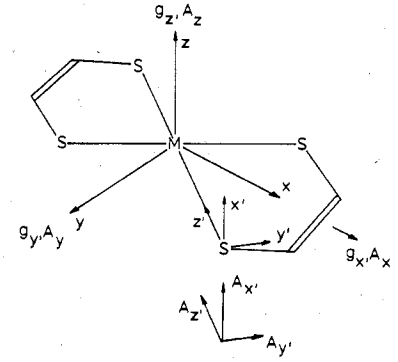

Figure 4. Coordinate system used for the EHT–MO calculations and orientations of the principal axes of the **g**, **A**, and ^{33}S hfs tensors in the MS_4 coordination sphere.

Schrauzer reported a b_{2g} orbital as the lowest unoccupied one for bis(ethylenedithiolato)nickel; in the case of the Ni(III) chelate this would be the orbital of the odd electron.

In order to interpret the experimental EPR parameters from the theoretical point of view, we made EHT calculations on [Ni(mnt)$_2$]$^-$. The computer program was based on the self-consistent charge and configuration method.[37] The SCCC iterations refer only to the Ni atom, considering the ligand atoms to be neutral. Slater-type orbitals were used for the radial part of the atomic wave functions.[38-40] The diagonal elements of the Hamiltonian matrix were approximated by the negative VOIP's (valence orbital ionization potentials).[41] The off-diagonal elements were described by the Wolfsberg–Helmholz relation.[42] In order to account the interatomic corrections, we used a screened Mulliken charge $q^x = kq$ with $0 \le k \le 1$. All computations were based on the structure of the bis(maleonitriledithiolato)nickel(III) monoanion[28,43] with an approximated D_{2h} symmetry. The coordinate system used is shown in Figure 4. The tensor elements were calculated according to the formulas given by Keijzers et al.[44] including all contributions arising from the metal and the sulfur atoms.

To find out the best conditions for obtaining the theoretical EPR parameters, we varied the constant F derived from the Wolfsberg–Helmholz relation from 1.8 to 2.7 and the parameter k from 0.0 to 1.0.

In all calculations the unpaired electron was found to be in a b_{2g} state. The best agreement between theoretical and experimental EPR quantities could be obtained for $k = 0.2$ and $F = 2.0$. However, there are still striking differences concerning the measured and the calculated **g**, $\mathbf{A}^{Ni}$, and $\mathbf{A}^{S}$ tensors which are listed in Table II. The calculated maximum g value points in the y direction, which is in agreement with the experiment. The main contribution to g_{yy} arises from occupied a_g MO's. The smallest theoretical **g** tensor component lies along the x axis while the experimental one points in the z position. **g** shifts for g_{zz} and g_{xx} are due to excitations to b_{3g} and b_{1g} states, respectively. All attempts made to change the directions of these axes by varying the parameters F and k were unsuccessful. However, this problem seems to be mainly caused by the calculated MO energies from which the excitation energies have to be derived which are necessary for the **g**-tensor calculation.

(30) R. Kirmse, B. V. Solovev, and B. G. Tarasov, *Ann. Phys. (Leipzig)*, **31**, 352 (1974).
(31) R. Kirmse, B. V. Solovev, and B. G. Tarasov, *Chem. Phys. Lett.*, **30**, 437 (1975).
(32) S. A. Altshuler, R. Kirmse, and B. V. Solovev, *J. Phys. C*, **8**, 1907 (1975).
(33) L. K. Aminov, R. Kirmse, and B. V. Solovev, *Phys. Status Solidi B*, **77**, 505 (1976).
(34) B. V. Solovev and R. Kirmse, *Fiz. Tverd. Tela*, **18**, 3094 (1976).
(35) I. N. Kurkin, Yu. K. Tchirkin, and V. I. Shlenkin, *Fiz. Tverd. Tela*, **14**, 2719 (1972).
(36) S. I. Shupack, E. Billig, R. J. H. Clark, R. Williams, and H. B. Gray, *J. Am. Chem. Soc.*, **86**, 4594 (1964).
(37) R. Hoffmann, *J. Chem. Phys.*, **35**, 149 (1961).
(38) J. Richardson, R. Powell, W. Nieuwpoort, and W. Edgell, *J. Chem. Phys.*, **36**, 1057 (1962).
(39) J. Richardson, R. Powell, and W. Nieuwpoort, *J. Chem. Phys.*, **38**, 796 (1963).
(40) E. Clementi and D. Raimondi, *J. Chem. Phys.*, **38**, 2686 (1963).
(41) H. Basch, A. Viste, and H. B. Gray, *Theor. Chim. Acta*, **3**, 458 (1965).
(42) M. Wolfsberg and L. Helmholz, *J. Chem. Phys.*, **20**, 837 (1952).
(43) C. J. Fritchie, Jr., *Acta Crystallogr.*, **20**, 107 (1966).
(44) C. P. Keijzers and E. de Boer, *Mol. Phys.*, **29**, 1007 (1975).

The anisotropic part of the ^{61}Ni hfs is in first-order axial symmetric with $A_{zz}^{Ni} = A_{xx}^{Ni} = 4.8 \times 10^{-4}$ cm^{-1} and $A_{yy}^{Ni} = -9.6 \times 10^{-4}$ cm^{-1} on the assumption of a negative sign for the nuclear magnetic moment. By addition of the second-order contributions, values are obtained which are listed in Table II. A rather good agreement with the anisotropic part of the experimental ^{61}Ni hfs can be reached only if the experimental A_{xx}^{Ni} component has a negative sign. However, a large part of the second-order contributions arises from the same excitations which are responsible for the **g**-tensor anisotropy. Therefore, it is questionable which of the small experimental A^{Ni} components has a negative sign because the calculated small **g**-tensor components do not agree with the experimental ones.

The calculated ^{33}S ligand hfs tensor is in reasonable agreement with the experimental one. According to the D_{2h} symmetry used for the calculations the ^{33}S hfs tensor is axial symmetric. The maximum component $A_{x'}^{S}$ lies perpendicular to the molecular plane. This is consistent with an out-of-plane π-bonding system involving the sulfur $p_{x'}$ orbitals.

Although the EHT calculations on $[Ni(mnt)_2]^-$ do not yield a complete description of the electronic properties of the molecule, the results help to interpret our experimental results. No attempts were made to perform EHT calculations on the Pd(III) and Pt(III) complexes. The results obtained by van Rens[45] and Nieuwpoort[46] for Ag(II), Au(II), and Mo(V) complexes show that the differences between calculated and measured EPR quantities are very large for heavier transition-metal ions.

Discussion

The experimental results outlined in the preceding section allow a determination of the directions of the principal axes of the **g**, the metal hfs, and the ^{33}S hfs tensors in the MS_4 unit of the complexes studied as given in Figure 4. From both the experimental data and the MO calculations we conclude that for these complexes the half-filled molecular orbital has b_{2g} symmetry being a linear combination of the metal d_{xz} orbital and the out-of-plane $3p_x$ orbitals of the four sulfur atoms mainly. An a_g ground state (D_{2h} symmetry) seems to be unlikely, because in this case ^{33}S hfs interactions should be measurable in the xy plane of the molecules.

For $[Ni(mnt)_2]^-$ the b_{2g} MO obtained by our EHT–MO calculations can be written as (contributions with LCAO coefficients ≤ 0.3 are neglected)

$$|b_{2g}\rangle = 0.33|d_{xz}(Ni)\rangle - 0.85\phi_{p_{x'}}(S) + 0.48\phi_{p_{x'}}(C_{ring})$$

The unpaired electron is largely delocalized over the ligand atoms: most of the unpaired spin density is found to be on the sulfur atoms. With use of eq 12 and the parameters[47] given in ref 7, the $3p_{x'}$ spin population on the S atoms can be estimated from the experimentally obtained axial component of the traceless ^{33}S hfs tensor. Neglecting the small hybridization between the S 3s and 3p orbitals the MO coefficient of the $3p_{x'}$ orbitals was found to be in the range 0.72–0.76 for the Ni(III) and Pd(III) complexes studied. This agrees with the S $3p_{x'}$ spin population calculated for $[Ni(mnt)_2]^-$.

It should be noted that, for the EHT–MO calculations, a rigorously planar complex ion with an approximated D_{2h} symmetry was assumed. Therefore, sulfur 3s orbitals do not contribute to the MO of the unpaired electron because of symmetry conditions. However, the experimentally obtained ^{33}S tensors show a small isotropic coupling $a_0^S = (A_{x'}^S + A_{y'}^S + A_{z'}^S)/3 = (7.8–9.5) \times 10^{-4}$ cm^{-1} on the assumption that the ^{33}S hfs tensor components are of the same sign. In principle the relative signs may be different ones. In such a case, however, very large values would be obtained for the spin densities on the sulfur atoms which disagree with those calculated by the MO method. Since the MO of the unpaired electron would then be entirely ligand in character, the metal hfs tensor cannot be explained. For the CuS_4-type chelates $(n\text{-}Bu_4N)[Cu(mnt)_2]$[48,49] and $Cu(Et_2dtc)_2$[50] (Et_2dtc = *N*,*N*-diethyldithiocarbamate), for which the complete ^{33}S hfs parameter sets (including a_0^S) have been obtained experimentally, all tensor components are of the same sign. These reasons make the above-made assumption concerning the relative signs of the ^{33}S tensor components for the $[M(mnt)_2]^-$ chelates reliable. Unfortunately, for these chelates the isotropic ^{33}S splitting could not be observed experimentally because the line widths in the liquid solution spectra are too large.

For $[Pt(dmi\text{-}t)_2]^-$ ^{33}S ligand hfs could not be observed in the spectra. However, since for $[Pt(mnt)_2]^-$ studied recently by us[12] the direction of the maximum component of the ^{33}S hfs tensor $A_{x'}^S$ as well as the magnitude of $A_{x'}^S$ shows the same behavior as observed for the analogous Ni(III) and Pd(III) complexes, there should be no striking differences concerning the bonding situation in the Pt(III) and the Ni(III) and Pd(III) complexes.

A comparison of the $A_{x'}^S$ values observed for the different Ni(III) and Pd(III) chelates shows a general tendency. In both cases the mnt chelates were found to have the largest $A_{x'}^S$ values, suggesting that among the complexes studied these chelates have the highest unpaired spin density on the sulfur atoms. The π-acceptor properties of the ligands should be mainly responsible for this ordering: because of the strong electron-drawing effect of the CN^- groups in contrast to the other two complex types in the mnt complexes, more electron density is expected to be in the out-of-plane ligand π-orbital system. This effect will be measurable from the magnitude of the axial ^{33}S hfs tensor components because they are mainly determined by the S $p_{x'}$ orbitals which participate in the out-of-plane π system. For Pt(III) chelates a similar behavior is expected although ^{33}S hfs data are available for $[Pt(mnt)_2]^-$ only. With comparison of the $A_{x'}^S$ values of the chelates $[Ni(mnt)_2]^-$, $[Pd(mnt)_2]^-$, and $[Pt(mnt)_2]^-$ a considerable increase is observed in the sulfur $3p_{x'}$ spin density in going from Ni to Pd. Between the Pd and the Pt chelate, however, the difference in $A_{x'}^S$ was found to be small.

Some comments should be made concerning the metal hfs. In the Ni(III) and Pd(III) chelates the maximum hfs component A_y was found to be coincident with g_y. As a striking difference to this for the Pt(III) complexes in the y direction, the smallest hfs component is observed. This is not unexpected since spin–orbit induced second-order contributions to A_y^{Pt} will be much more significant than for Ni(III) or Pd(III) complexes because of the large spin–orbit coupling constant of platinum. These contributions reach the magnitude of the first-order contributions and have the opposite sign; therefore, the resulting hfs will be small for this orientation. The signs of the hfs components are positive for the ^{105}Pd tensor and negative for the ^{195}Pt tensor because the nuclear magnetic moments were determined to be negative for ^{105}Pd and positive for ^{195}Pt, respectively.[51] The nuclear magnetic moment for

(45) J. G. M. van Rens, Thesis, University of Nijmegen, 1974.
(46) A. Nieuwpoort, Thesis, University of Nijmegen, 1975.
(47) For the expectation value we used $\langle r^{-3}\rangle_{3p} = 31.2 \times 10^{24}$ cm^{-3} (taken from J. R. Morton, *Chem. Rev.*, **64**, 454 (1964)).
(48) R. Kirmse, J. Stach, W. Dietzsch, and E. Hoyer, *Inorg. Chim. Acta*, **26**, L 53 (1978).
(49) From our measurements on carefully degassed acetone solutions of $(n\text{-}Bu_4N)_2[^{63}Cu(mnt)_2]$ a value of $a_0^S = 12.1 \times 10^{-4}$ cm^{-1} has been obtained for the isotropic ^{33}S splitting.
(50) R. Kirmse and B. V. Solovev, *J. Inorg. Nucl. Chem.*, **39**, 41 (1977).
(51) A. Abragam and B. Bleaney, "Electron Paramagnetic Resonance of Transition Ions", Clarendon Press, Oxford, 1970, Chapter 7.

^{61}Ni was assumed to be negative.

The line widths observed in the single-crystal spectra are very small even at room temperature. The contributions to the line width which must be considered are (a) unresolved ligand hfs interactions, (b) electron spin–lattice relaxation processes, and (c) small lattice distortions giving rise to a distribution of the paramagnetic molecules over a small range of orientations. The room-temperature line width estimated from the relaxation data for $(n\text{-}Bu_4N)[Ni/Au(mnt)_2]$ agrees very well with the experimental one. A similar good agreement was observed for $(n\text{-}Bu_4N)[Pt/Au(mnt)_2]$.[12] In the latter case the Raman relaxation rate is faster, which results in a larger line width than observed for the Ni(III) complex. Therefore, spin–lattice interactions are mainly responsible for the room-temperature line width. An additional line width contribution can be caused by hyperfine interactions with protons of the $(n\text{-}Bu_4N)^+$ counterions or with ligand protons for the xdt systems. In the mnt complexes these interactions will not give a noticeable contribution because of the large metal–proton distances. For the xdt or dmi-t complexes a small contribution of approximately 10^{-4} cm^{-1} can be observed from the counterion protons if the $(n\text{-}Bu_4N)^+$ groups are placed in the fifth and/or sixth coordination positions of the coordination sphere. Unfortunately, no structural data are available for these complexes. Line width contributions arising from lattice distortions can be considered as being very small for the mnt and dmi-t chelates since no line width variation was observed when the crystals were rotated. The xdt chelates show a small line width variation; however, since the structure of $(n\text{-}Bu_4N)[Cu(xdt)_2]$ is unknown, this variation cannot be attributed unambiguously to lattice distortions without consideration of unresolved proton hyperfine interactions.

The long spin–lattice relaxation times (T_1(300 K) $\approx$ 10^{-6}–10^{-7} s) are the result of (a) a low value of the Debye temperature and (b) the high metal–ligand covalency in the molecules of these molecular crystals. Analogous[30-34] results have been obtained from experimental and theoretical relaxation studies on copper(II) bis(dialkyldichalcogenocarbamates) which are similar to the dithiolene chelates concerning their bonding properties.

Preliminary crystal structure work on $(n\text{-}Bu_4N)[Au(mnt)_2]$ has shown that this complex is isomorphous with the analogous Cu(III) complex. Therefore, it is not surprising that weak metal–metal pair lines appear in the EPR spectra even for higher doped crystals. From the relaxation experiments the pair relaxation rate was found to be greater than the relaxation rate of the "single Ni^{3+} ions". This is not unexpected since due to the greater number of energy levels present in pairs there exist more possibilities for the energy transfer from the pairs to the lattice than for "single ions". As a result, pairs relax faster than "single ions".[32]

Acknowledgment. We wish to thank Professor Dr. S. A. Altshuler and Dr. B. V. Solovev (Physics Department, State University, Kazan, USSR) for their help in measuring the relaxation data. We are indebted to Dr. S. Wartewig (Physics Department, Karl Marx University, Leipzig) and to Dr. J. Sieler (Chemistry Department, Karl Marx University, Leipzig) for helpful discussions concerning the MO calculations and for communication of preliminary crystal structure data of $(n\text{-}Bu_4N)[Au(mnt)_2]$.

Registry No. $(n\text{-}Bu_4N)[Ni(dmi\text{-}t)_2]$, 68401-88-7; $(n\text{-}Bu_4N)[Pd(dmi\text{-}t)_2]$, 73712-40-0; $(n\text{-}Bu_4N)[Pt(dmi\text{-}t)_2]$, 73712-42-2; $(n\text{-}Bu_4N)[Au(dmi\text{-}t)_2]$, 73712-44-4; $(n\text{-}Bu_4N)[Ni(mnt)_2]$, 18958-62-8; $(n\text{-}Bu_4N)[Ni(xdt)_2]$, 15338-39-3; $(n\text{-}Bu_4N)[Pd(xdt)_2]$, 73712-46-6; $(n\text{-}Bu_4N)[Au(mnt)_2]$, 14710-21-5; $(n\text{-}Bu_4N)[Cu(xdt)_2]$, 15442-44-1; $(n\text{-}Bu_4N)_2[Ni(dmi\text{-}t)_2]$, 72022-67-4; $(n\text{-}Bu_4N)_2[Pd(dmi\text{-}t)_2]$, 72688-90-5; $(n\text{-}Bu_4N)_2[Pt(dmi\text{-}t)_2]$, 72688-91-6; $C_3S_5(COC_6H_5)_2$, 68494-08-6; $HAuCl_4$, 16903-35-8.

Contribution from the Research Institute for Materials, University of Nijmegen, Toernooiveld, 6525 ED Nijmegen, The Netherlands

$^{31}P[^1H]$ Nuclear Magnetic Resonance Investigation of Gold Cluster Compounds

F. A. VOLLENBROEK, J. P. VAN DEN BERG, J. W. A. VAN DER VELDEN, and J. J. BOUR*

Received October 17, 1979

$^{31}P[^1H]$ NMR spectra of gold–phosphine clusters—$Au_8(PAr_3)_8^{2+}$, $Au_9(PAr_3)_8^{3+}$, $Au_{11}(PAr_3)_7X_3$, and $Au_{11}(PAr_3)_8Y_2^+$ (X = SCN, I; Y = SCN, Cl)—show only one singlet, which is explained by a dominant trans influence of the central gold atom upon the chemical shifts of the phosphines coordinated to peripheral gold atoms. $Au_{11}[P(p\text{-}ClC_6H_4)_3]_7(SCN)_3$–$PPh_3$ mixtures in C_6D_6 show a complex pattern which is interpreted as the result of the presence of $Au_{11}L'_{7-n}L_n(SCN)_3$ clusters (L′ = $P(p\text{-}ClC_6H_4)_3$, L = PPh_3, $0 \leq n \leq 7$) in which different phosphines are coordinated to one cluster. Spectra of $Au_{11}L'_{7-n}L_n(SCN)_3$ (n = 0–2) mixtures can be interpreted by assuming that L couples with all L′ phosphines with the same coupling constant. From this it is concluded that the coupling is mainly transmitted through the central gold atom.

Introduction

In the course of our work on gold clusters, chemical analyses and conventional spectroscopic methods (e.g., IR) were found to be of limited use to identify and to verify purity of gold clusters. ^{31}P NMR spectroscopy, however, proved to be very useful and became the main analytical tool in our work. This technique was also used to investigate reactions of gold–phosphine clusters[1-3] and to obtain information about chemical bonding and dynamical properties of these compounds.

Experimental Section

The following gold clusters were prepared according to known procedures: $Au_8(PAr_3)_8^{2+}$ by the reaction of $Au_9(PAr_3)_8^{3+}$ with an excess of PAr_3;[2] $Au_9(PAr_3)_8^{3+}$ by the reduction of $Au(PAr_3)NO_3$ with $NaBH_4$;[5] $Au_{11}(PAr_3)_7X_3$ by the reduction of $Au(PAr_3)X$ with $NaBH_4$;[4] $Au_{11}(PAr_3)_8Y_2^+$ by the reaction of $Au_9(PAr_3)_8^{3+}$ with Y^-.[1] ^{31}P NMR

(1) F. A. Vollenbroek, J. J. Bour, J. M. Trooster, and J. W. A. van der Velden, *J. Chem. Soc., Chem. Commun.*, 907 (1978).
(2) F. A. Vollenbroek, W. P. Bosman, J. J. Bour, J. H. Noordik, and P. T. Beurskens, *J. Chem. Soc., Chem. Commun.*, 387 (1979).
(3) F. A. Vollenbroek, Thesis, Nijmegen, 1979, and to be submitted for publication.
(4) F. Cariati and L. Naldini, *Inorg. Chim. Acta*, **5**, 172 (1971).
(5) F. Cariati and L. Naldini, *J. Chem. Soc., Dalton Trans.*, 2286 (1972).
(6) F. A. Vollenbroek, P. C. P. Bouten, J. M. Trooster, J. P. van den Berg, and J. J. Bour, *Inorg. Chem.*, **17**, 1345 (1978).

0020-1669/80/1319-2685$01.00/0